A High-Resolution ^{17}O and ^{29}Si NMR Study of Zeolite Siliceous Ferrierite and ab Initio Calculations of NMR Parameters

L. M. Bull,*,† B. Bussemer,‡ T. Anupõld,§ A. Reinhold,§ A. Samoson,§ J. Sauer,‡ A. K. Cheetham,⊥ and R. Dupree||

Contribution from the Institut des Matériaux Jean Rouxel, 2 rue de la Houssinière, B.P. 32229, 44322 Nantes, Cedex 3, France, Humboldt-Universität, Institut für Chemie, Berlin, D-10117, Germany, National Institute of Chemical Physics and Biophysics, Akadeemia Tee 23, Tallinn, Estonia, Materials Research Laboratory, University of California, Santa Barbara, California 93106, and Physics Department, University of Warwick, Coventry, U.K.

Received September 14, 1999. Revised Manuscript Received January 3, 2000

Abstract: High resolution ^{17}O NMR spectra of siliceous ferrierite (Sil-FER) have been collected and the ^{29}Si and ^{17}O isotropic chemical shifts and the electric field gradients of oxygen have been calculated from first principles. The theoretical ^{29}Si MAS NMR spectrum is found to be in excellent quantitative agreement with the experimentally determined spectrum, and is extremely sensitive to the accuracy of the structure used for the calculations, thus providing a method for assessing the quality of the structure determination. However, theoretical predictions of the chemical shifts, quadrupolar coupling constants and asymmetry parameters show only qualitative agreement with the experimental ^{17}O NMR spectra obtained by Double Rotation (DOR) and multiple quantum magic angle spinning (MQMAS) as the spectra are much more complex (10 peaks within a shift range of less than 15 ppm, and the quadrupolar coupling constants only differ by 0.4 MHz) and hence higher accuracy is required from the shift calculations (>0.5 ppm), which is currently not possible. These findings also demonstrate the current limitations of the experimental techniques and show that no simple correlation appears to exist between the zeolite structure, such as the Si−O−Si bond angles or lengths, and the ^{17}O NMR parameters.

1. Introduction

^{29}Si and ^{27}Al solid-state NMR have already played a vital role in the characterization of zeolitic materials,[1] allowing the determination of, for example, the number of crystallographic sites in a structure,[2] their relative proportions and their connectivities,[3] the coordination environments of the sites and hence the degree of condensation of the framework,[4] and the silicon-to-aluminum ratio.[5] By contrast, relatively few ^{17}O NMR studies have been performed. This is due to the problems arising from its low natural abundance (0.037%) combined with its small magnetic moment and the high cost of enrichment, and its relatively large electric field gradient in silicates that often causes the static and magic-angle spinning line shapes to be broad and featureless.[6,7] However, ^{17}O NMR has the potential to be a highly sensitive structural probe of zeolitic materials because oxygen (i) has the largest framework ionic radius, and hence it is the framework atom most intimately involved in adsorption and catalytic processes, and (ii) is a quadrupolar nucleus and thus both the chemical shift and electric field gradient tensors can be exploited. Building on earlier work,[8] recent developments in NMR experimentation have led to much increased interest in this nucleus.[9−11] For example, we have recently demonstrated that using high magnetic field strengths (11.7−16.85 T) and state-of-the-art double rotation probes, all crystallographically inequivalent oxygen sites could be resolved for the first time in a zeolite (the four sites of the silica polymorph of faujasite, Sil-Y).[11] While semiempirical correlations based on the Townes−Dailey model[12,13] between the bond angle at oxygen and either the quadrupolar coupling constant, C_Q, or the asymmetry parameter of the electric field gradient, η, have been used to assign spectra, others[14] have tried to gain a better understanding of correlations between ^{29}Si and ^{17}O NMR properties and local structural parameters by performing calculations on a number of silicate clusters that in principle serve as models for SiO_4

† Institut des Matériaux Jean Rouxel.
‡ Institut für Chemie.
§ National Institute of Chemical Physics and Biophysics.
⊥ University of California.
|| University of Warwick.

(1) Engelhardt, G.; Michel, D. *High-Resolution Solid-State NMR of Silicates and Zeolites*; Wiley: Chichester, 1987.
(2) Fernandez, C.; Amoureux, J. P.; Chezeau, J. M.; Delmotte, L.; Kessler, H. *Microporous Mater*. **1996**, *6*, 331−340.
(3) Fyfe, C. A.; Gies, H.; Feng, Y.; Kokotailo, G. T. *Nature* **1989**, *341*, 223−225.
(4) Koller, H.; Wolker, A.; Eckert, H.; Panz, C.; Behrens, P. *Angew. Chem. Int. Ed.* **1998**, *36*, 2823−2825.
(5) Engelhardt, G.; Lohse, U.; Lippmaa, E.; Tarmak, M.; Magi, M. *Z. Anorg. Allg. Chem.* **1981**, *482*, 49.
(6) Mueller K. T.; Wu Y.; Chmelka B. F.; Stebbins J.; Pines, A. *J. Am. Chem. Soc.* **1991**, *113*, 32−38.
(7) Timken, H. K. C.; Janes, N.; Turner, G. L.; Lambert, S. L.; Welsh, L. B.; Oldfield, E. *J. Am. Chem. Soc.* **1986**, *108*, 7236−7241.
(8) Schramm, S.; Oldfield, E. *J. Am. Chem. Soc*. **1984**, *106*, 2502−2506.
(9) Pingel, U. T.; Amoureux, J. P.; Anupold, T.; Bauer, F.; Ernst, H.; Fernandez, C.; Freude, D.; Samoson, A. *Chem. Phys. Lett*. **1998**, *294*, 345−350.
(10) Stebbins, J. F.; Lee, S. K.; Oglesby, J. V. *Am. Min*. **1999**, *84*, 983−986.
(11) Bull, L. M.; Cheetham, A. K.; Anupold, T.; Reinhold, A.; Samoson, A.; Sauer, J.; Bussemer, B.; Lee, Y.; Gann, S.; Shore, J.; Pines, A.; Dupree, R. *J. Am. Chem. Soc.* **1998**, *120*, 3510−3511.
(12) Grandinetti, P. J.; Baltisberger, J. H.; Farnan, I.; Stebbins, J. F.; Pines, A. *J. Phys. Chem*. **1995**, *99*, 12341−12348.
(13) Townes, C. H.; Dailey, B. P. *J. Chem. Phys*. **1949**, *17*, 782.
(14) Xue, X.; Kanzaki, M. *Chem. Mineral*. **1998**, *26*, 14−30.

10.1021/ja993339y CCC: $19.00
Published on Web 05/04/2000

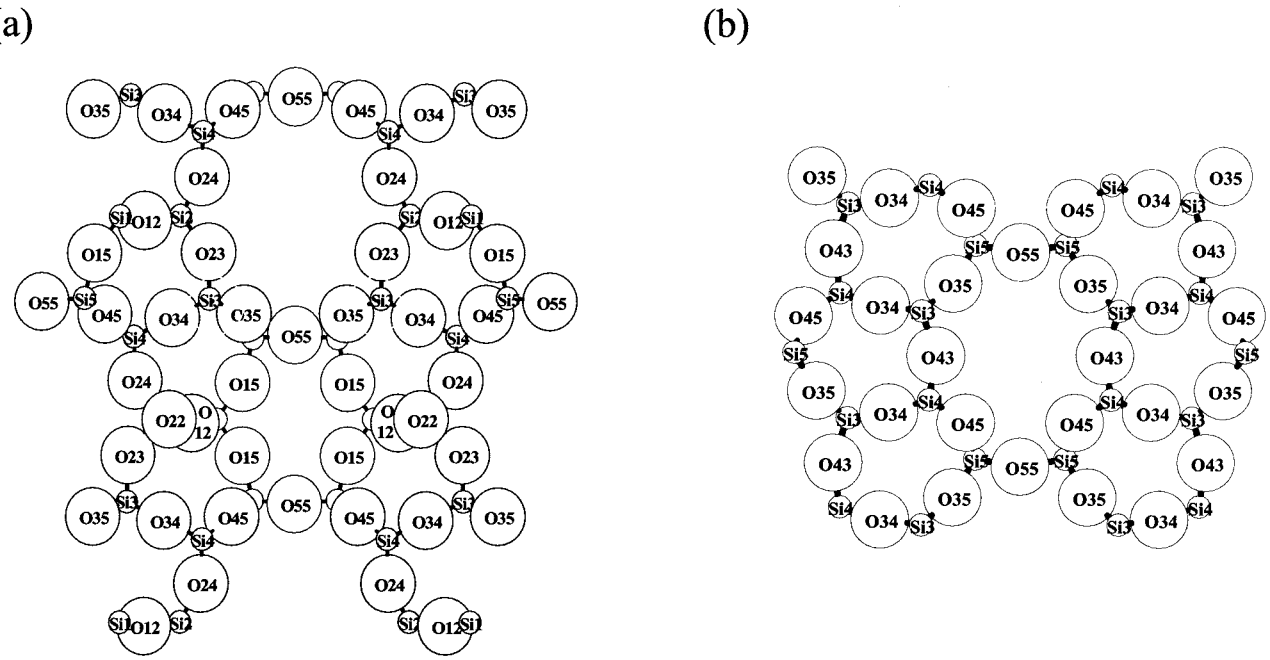

Figure 1. The structure of Sil-FER (space group *Pnnm*) viewed along the (a) [100] and (b) [010] directions showing respectively the 10- and 8-ring channels.

tetrahedra in silicate minerals. We too have used quantum mechanical chemical shift and field gradient calculations, but using clusters sufficiently large as to represent the local environment of the nucleus at the center. Our confidence in this latter method of assignment is based upon the fact that the assignment of Sil-Y remains unchanged when parameters of the computational approach are varied, such as the basis set used, the size of the cluster (above 3 coordination shells for oxygen), and the computational method applied.[15] In this paper we first demonstrate that it is possible to obtain high-resolution ^{17}O NMR spectra from a complex zeolite structure, Sil-FER,[16] which has 10 crystallographically distinct oxygen sites, and then we attempt to assign the spectrum based upon first principles calculations of the NMR parameters. We will show from ^{29}Si and ^{17}O NMR chemical shielding calculations that the availability of an accurate structure determination from neutron or X-ray diffraction is essential for the calculations to reliably reproduce the observed NMR spectrum.

It should be emphasized at this point that the methods presented here are equally applicable to other oxide materials including inorganic, biological, and organic/inorganic hybrid compounds, where the interpretation of the NMR spectra could be essential for understanding the relationships between subtle structural features and properties. This paper demonstrates that the NMR experiments and quantum chemical shift calculations can determine which crystal structure more closely represents the local environment as probed by NMR, and that subtle differences between a single crystal and a powder structure determination are important enough to completely change the NMR spectrum.

Comparison of Two Siliceous Ferrierite Structures. The zeolite ferrierite is well-known both in nature and as a synthetic material.[17] Current interest in the aluminum-containing phase has been stimulated by a report that it is an excellent shape-selective catalyst for the isomerization of *n*-butenes to isobutene.[18] The latter is an important feedstock for the production of methyl *tert*-butyl ether (MTBE), which is a commercial oxygenate additive in motor fuel. Ferrierite has also shown potential as a deNOx catalyst for car exhaust systems.[19] Ferrierite is normally synthesized as an aluminosilicate with Na,K counterions and the structure has been typically refined in the space group *Immm*, which leads to a symmetry imposed and highly questionable 180° Si−O−Si bond angle.[20] However, a single crystal study by Gramlich-Meier et al.[21] found evidence for lowering the symmetry from orthorhombic to the monoclinic space group $P2_1/n$.

More recently, Kuperman and co-workers[22] have demonstrated that relatively large single crystals of all-silica ferrierite can be synthesized using a nonaqueous fluoride-containing reaction mixture. The space group was reported to be *Pnnm* with 5 Si sites and 10 oxygen sites, but a full structural determination was not presented. Morris et al.[23] and Lewis et al.[24] have since published detailed crystal structures in the space group *Pnnm*. For the remainder of this paper these publications will be referred to as simply Morris and Lewis, respectively. The ^{29}Si MAS NMR spectra of the samples from Morris and Lewis clearly show the presence of five peaks in the correct proportions (4:8:8:8:8), and Morris also used the combination of a 2-D INADEQUATE experiment and correlations between the average function ($\cos\alpha/\cos\alpha - 1$) for each Si site (where α = Si−O−Si bond angle) and the chemical shift to successfully assign the spectrum to the structure in space group *Pnnm*.

Figure 1 shows the structure of Sil-FER (*Pnnm* symmetry)

(15) Bussemer, B., Ph.D. Thesis, Humboldt-Universität, Berlin, 2000.
(16) Meier, W. M.; Olson, D. H.; Baerlocher, Ch. In *Atlas of zeolite structure Types*; Elsevier: London, 1996; p 106.
(17) Wise, W. S.; Tschernich, R. W. *Am. Mineral.* **1976**, *61*, 60.
(18) Haggin, J. *C&EN* **1993**, *October 25*, 30.
(19) Attfield, M. P.; Weigel, S. J.; Cheetham, A. K. *J. Catal.* **1997**, *172*, 274−280.
(20) Vaughan, P. A. *Acta Crystallogr.* **1966**, *21*, 983.
(21) Gramlich-Meier, R.; Gramlich, V.; Meier, W. M. *Am. Chem. Mineral.* **1985**, *119*, 261.
(22) Kuperman, A.; Nadimi, S.; Oliver, S.; Ozin, G. A.; Garces, J. M.; Olken, M. M. *Nature* **1993**, *97*, 239−242.
(23) Morris, R. E.; Weigel, S. J.; Henson, N. J.; Bull, L. M., Janicke, M. T., Chmelka, B. F.; Cheetham, A. K. *J. Am. Chem. Soc.* **1994**, *116*, 11849−11855.
(24) Lewis, J. E.; Freyhardt, C. C.; Davis, M. E. *J. Phys. Chem.* **1996**, *100*, 5039−5049.

Table 1. Comparison of the Bond Angles and Lengths for the Structures of Sil-FER[a]

	Lewis	Morris		Lewis	Morris		Lewis	Morris
				bond angles (deg)				
Si1−O12−Si2	156.6(2)	153.7(8)	Si3−O23−Si2	144.9(8)	142.2(8)	Si3−O43−Si4	148.1(2)	149.5(6)
Si1−O15−Si5	155.4(2)	156.8(6)	Si3−O35−Si5	143.7(1)	138.3(8)	Si4−O45−Si5	164.5(2)	161.3(9)
Si2−O22−Si2	149.1(3)	144.7(8)	Si3−O34−Si4	167.4(2)	170.7(9)	Si5−O55−Si5	158.3(2)	159.5(14)
Si2−O24−Si4	153.0(2)	152.4(9)						
				bond lengths (Å)				
Si1−O15	1.585(2)	1.581(8)	Si3−O35	1.594(2)	1.584(11)	Si4−O43	1.599(2)	1.643(14)
Si1−O12	1.595(2)	1.609(8)	Si3−O43	1.600(2)	1.559(14)	Si4−O24	1.601(2)	1.593(14)
Si2−O24	1.591(2)	1.572(15)	Si3−O34	1.600(2)	1.586(14)	Si5−O55	1.5913(9)	1.593(5)
Si2−O12	1.593(3)	1.585(8)	Si3−O23	1.605(2)	1.625(14)	Si5−O45	1.593(2)	1.637(12)
Si2−O22	1.596(1)	1.632(15)	Si4−O45	1.581(2)	1.625(12)	Si5−O15	1.597(2)	1.594(8)
Si2−O23	1.597(2)	1.652(5)	Si4−O34	1.592(2)	1.573(13)	Si5−O35	1.602(2)	1.563(12)

[a] The atom labels follow those given in Figure 1.

viewed along the [001] and the [010] directions. The atoms are labeled according to Lewis, where, for example, O45 is the oxygen bridging Si4 and Si5. The structure of FER is based on 5-ring building units that are connected to form oval 10-ring channels running parallel to [001], and these are intersected by 8-ring channels running parallel to [010]. Table 1 lists the bond angles and bond lengths for the two structures of Sil-FER. The structure of Lewis is more accurate than that of Morris; for example, the spread of Si−O bonds is much greater in the Morris structure than in that of Lewis. This is not surprising since the former was obtained from powder X-ray and neutron diffraction, whereas the latter was based on a single-crystal X-ray determination.

Another qualitative assessment of silica polymorph crystal structures, which was proposed by Cheetham, Bull and Henson,[25] involves comparing the goodness-of-fit to the well-known semiempirical correlation between the ^{29}Si NMR isotropic shifts and the average Si−O−Si angle for each Si site (see above).[26] This correlation is based on the approximately linear relationship between the ^{29}Si NMR chemical shift and the electronegativity of the bonding oxygen since the electronegativity of the oxygen is related to the degree of s hybridization of the oxygen bonding orbitals, and the latter is related to the Si−O−Si bond angle. Figure 2 shows such a plot for the two experimental structures (filled symbols). The ^{29}Si NMR chemical shifts for the samples of Lewis and Morris are taken from the literature and, as expected, are very similar. To be able to judge the goodness of fit of the data, we have superimposed a line that is the fit to data taken from Fyfe et al.[27] for silicalite (Si-MFI), which gives an excellent correlation for this function. Again, it is clear that the accuracy of the structure of Lewis is superior to that of Morris (see correlation coefficients in the insert of Figure 2).

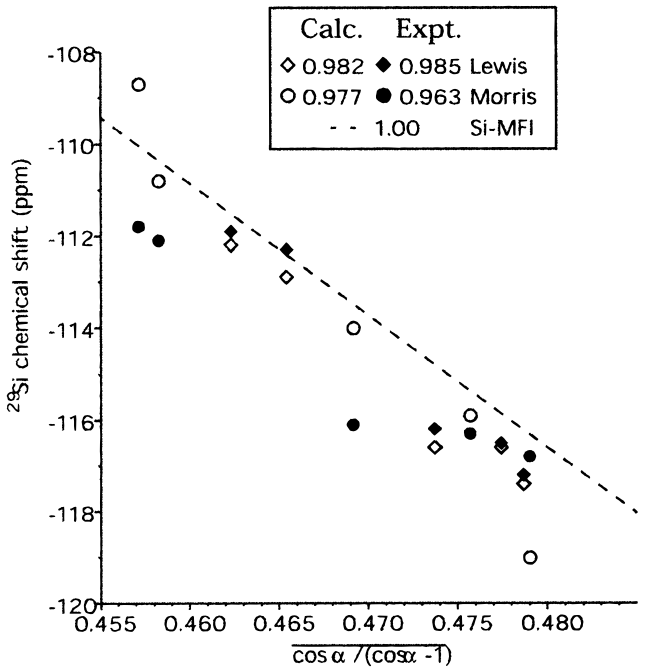

Figure 2. Semiempirical correlation between the experimental (filled symbols) and calculated (open symbols) ^{29}Si NMR chemical shift and the function $\overline{\cos\alpha/(\cos\alpha-1)}$, where there are four Si−O−Si angles, α, around each Si site. The dashed line represents the best fit to the ^{29}Si NMR results of Fyfe et al.[27] for siliceous ZSM-5 (Si-MFI). Correlation coefficients are given for each data set in the insert.

2. NMR Experiments

The observed ^{17}O NMR isotropic shift arises from the summation of two components, the isotropic chemical shift, δ_{iso}^{cs} and the isotropic second-order quadrupolar shift, δ_{iso}^{2Q}. The chemical shift is field independent, but δ_{iso}^{2Q} of the central transition for a nucleus with spin I is equal to:

$$\delta_{iso}^{2Q} = -{}^{3}/_{40}(C_Q/\upsilon)^2[(I(I+1) - {}^{3}/_{4})/I^2(2I-1)^2](1+\eta^2/3)$$

where υ is the Larmor frequency of the nucleus. From the field dependence of the observed DOR shift, δ_{iso}^{cs} can be extracted from the intercept and the quadrupolar product, $P_Q = C_Q(1+\eta^2/3)^{1/2}$, from the gradient. The MQMAS data can be used in the same plot once the Larmor frequency has been adjusted to compensate for the quadrupolar interaction of the higher quantum transitions shifting the observed peaks to high frequencies by a factor of 17/10 compared to the single quantum central transition. Hence, the DOR shifts are plotted versus $1/\upsilon^2$ whereas the MQMAS data are plotted versus $-(10/17)/\upsilon^2$.[28]

The double rotation (DOR)[29] spectra of Sil-FER were collected at 14.04, 17.6, and 18.7 T on Bruker DMX spectrometers located at the National High Magnetic Field Laboratory, Tallahassee, FL, Technical University of Munich, Germany, and the Frankfurt University Center for Biomolecular NMR, Germany, respectively. The spectra at 11.7 and 16.85 T were collected on Varian Unity spectrometers again at the NHMFL. Home-built DOR probes were used. Regulation of the four air pressures was performed by a home-built spin controller connected to an SGI for monitoring the inner and outer rotor speeds.[30] All spectra were collected by synchronizing the excitation pulse with

(25) Cheetham, A. K.; Bull, L. M.; Henson, N. J. *Stud. Surf. Sci. Catal.* **1997**, *105*, 2267−2274.
(26) Engelhardt, G.; Radeglia, R. *Chem. Phys. Lett.* **1984**, *108*, 271−274.
(27) Fyfe, C. A.; Feng, Y.; Grondey, H. *Microporous Mater.* **1993**, *1*, 393−400.
(28) Anupõld, T.; Reinhold, A.; Sarv, P.; Samoson, A. *Solid State NMR* **1998**, *13*, 87−91.
(29) Chmelka, B. F.; Zwanziger, J. W. *NMR Basic Principles and Progress*; Springer-Verlag: Berlin, 1994; Vol. 33, pp 79−124.

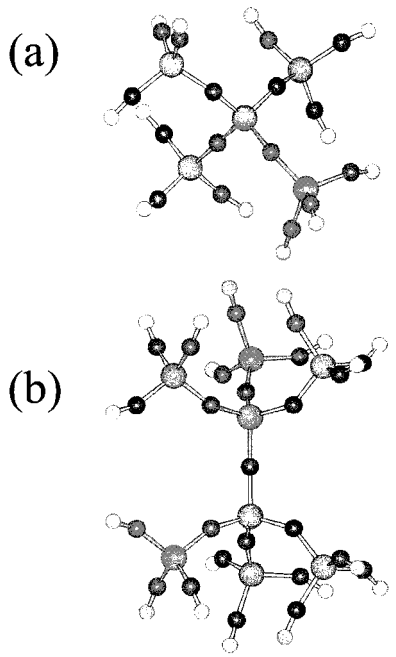

Figure 3. Examples of how clusters are constructed for the central atoms: (a) shell-3 cluster for silicon and (b) shell-4 cluster for oxygen.

the position of the outer rotor.[31] Typically the repetition time between scans was 1 s. All spectra were referenced to liquid water at 0 ppm.

The 2D split-t_1 3Q MQMAS experiment[32] was performed on a Varian CMX Infinity 600 spectrometer at Warwick University, U.K., operating at a frequency of 81.3566 MHz for ^{17}O. A Varian/Chemagnetics 4 mm double bearing MAS probe was used. The sample was spun at 15 kHz in a zirconia rotor. 768 scans were acquired for each t_1 slice using a repetition time of 1 s. Data were collected to 28.7 ms using a dwell time of 100 μs in the indirectly detected dimension. The data were referenced to liquid water at 0 ppm in both dimensions and then the t_1 dimension was scaled by 17/31.[33] Simulations of the line shape of each peak were performed with the Bruker WINFIT[34] program using 5 Hz of Lorentzian line broadening and the C_Q and η values were constrained to the P_Q values obtained from the DOR data.

3. Sample Preparation

Sil-FER was synthesized according to the method of Kuperman et al.[22] and Morris.[23] The organics trapped within the structure were removed by calcination using a 99% oxygen atmosphere in a Lindberg muffle furnace, which was ramped at 2 °C/min from room temperature to 850 °C, where it was held for 16 h. The resulting calcined Sil-FER was white and showed no evidence of occluded carbon. The sample was then placed in a thick-walled quartz tube, evacuated at room temperature (10^{-5} Torr), and then 1/3 atm of $^{17}O_2$ gas (37% $^{17}O_2$) was added. After the tube was closed it was heated to 750 °C (ramp 5 °C/min) and held at this temperature for 18 h. The structure of the resulting enriched material was verified to be ferrierite. No degradation of the crystallinity was apparent by X-ray diffraction.

4. Quantum Chemical Calculations

Models and Methods. Only recently has a periodic code for the calculation of NMR shieldings been developed[35] and applied to carbon nitride compounds.[36] It is based on density functional theory and uses plane wave basis sets along with a pseudopotential representation of the atomic cores. We make use of an alternative approach and apply molecular codes to cluster models for the different atomic sites of the material. Previous studies on silica and zeolites[15,37−39] as well as on carbon and silicon nitrides[40] have demonstrated that because the NMR chemical shift is a local probe of the structure the use of cluster models for quantum mechanical calculations of the shielding constants is a relatively accurate method if the clusters are sufficiently large.[15,37] For the present study, models for the clusters are cut from a given periodic structure; they are constructed for every crystallographically inequivalent site, with the site of interest at the center and with coordination spheres of increasing size built around it (see Figure 3 for examples). The size of the cluster is defined by the number of coordination shells surrounding the central atom, i.e., a shell-2 model with a central atom of silicon will consist of the central atom surrounded by a first coordination shell of oxygen and then a second coordination sphere of silicon. The clusters are then terminated with hydrogen atoms that replace, in the example of the shell-2 model, the third coordination sphere of oxygen, i.e., the original O−Si−O angle is maintained, but the edge atom−proton distance is reduced to 0.95 Å for O and 1.483 Å for Si, values that have been obtained from Hartree−Fock (HF) calculations.[37]

Ab initio calculations of the NMR shielding constants were performed principally using the coupled perturbed HF method (unless stated otherwise)[41−43] using the Sheila module of the TURBOMOLE code.[43] This is a standard technique for calculating shielding constants for molecules. Field-dependent basis functions (gauge including atomic orbitals) were explicitly used as suggested by Ditchfield.[41] To check the dependence of the ^{17}O chemical shift results on the method used, density functional (DF) chemical shifts were calculated with the GAUSSIAN program using the B3LYP functional.[44]

^{29}Si NMR Isotropic Chemical Shifts. Calculations of ^{29}Si NMR chemical shifts were performed using shell-3 clusters (Figure 3a) cut from the different ferrierite framework structures. Generally a triple-ζ plus polarization (TZP) basis set was used for oxygen and a double-ζ plus polarization (DZP) basis set was applied to silicon and the terminating hydrogen atoms. This use of mixed basis sets for a cluster, which we define as T(O)-DZP, accounts for the fact that oxygen is the electronegative component in SiO_2. All basis sets were taken from the Karlsruhe library of fully optimized (using analytical gradients) basis sets.[45] It has been demonstrated that the combination of these parameters leads to quantitatively accurate results for a series of zeolites.[37]

α-Quartz was used as an internal secondary shift standard for the calculations. Calculated absolute isotropic shielding constants, σ, were converted to relative shifts, δ, with respect to TMS using the formula:

(30) Developed at the National Institute of Chemical Physics and Biophysics, Tallinn, Estonia.

(31) Samoson, A.; Lippmaa, E. *J. Magn. Reson.* **1989**, *84*, 410−416.
(32) Brown, S. P.; Wimperis, S. *J. Magn. Reson.* **1997**, *124*, 279−285.
(33) Man, P. *Phys. Rev. B* **1998**, *58*, 2764−2782.
(34) WinFit written and developed by D. Massiot, CNRS, Orleans, France.
(35) Mauri, F.; Pfrommer, B. G.; Louie, S. G. *Phys. Rev. Lett.* **1996**, *77*, 5300−5303.
(36) Yoon, Y.-G.; Pfrommer, B. G.; Mauri, F.; Louie, S. G. *Phys. Rev. Lett.* **1998**, *80*, 3388−3391.
(37) Bussemer, B.; Schröder, K.-P.; Sauer, J. *Solid State NMR* **1997**, *9*, 155−164.
(38) Valerio, G.; Goursot, A.; Vetrivel, A.; Malkina, O.; Malkin, V.; Salahub, D. R. *J. Am. Chem. Soc.* **1998**, *120*, 11426−11431.
(39) Valerio, G.; Goursot, A. *J. Phys. Chem. B* **1999**, *103*, 51−58.
(40) Tossell, J. A. *J. Magn. Reson.* **1997**, *127*, 49−53.
(41) Ditchfield, R. *Mol. Phys.* **1974**, *27*, 789.
(42) Wolinski, K.; Hinton, J.; Pulay, F. P. *J. Am. Chem. Soc.* **1990**, *112*, 8251−8260.
(43) Häser, M.; Ahlrichs, R.; Baron, H. P.; Weis, P.; Horn, H. *Theor. Chim. Acta* **1992**, *83*, 455−470.

$$\delta_{TMS}(\text{cluster}) = \sigma(\alpha\text{-quartz}) + \delta_{TMS}(\alpha\text{-quartz}) - \sigma(\text{cluster})$$

The observed chemical shift for α-quartz, $\delta_{TMS}(\alpha\text{-quartz}) = -107.4$ ppm,[46] was used to reference the internal α-quartz shifts, $\sigma(\alpha\text{-quartz})$, to TMS. The calculated shielding value for $\sigma(\alpha\text{-quartz})$ was 495.14 ppm.

^{17}O NMR Isotropic Chemical Shifts. ^{17}O NMR chemical shift calculations were performed using shell-4 models (Figure 3b), except where noted otherwise. Three types of basis set combinations were investigated for calculating ^{17}O NMR shielding constants of Sil-FER, which are listed in Table 2. The total number of basis functions used for the shielding values of α-quartz are also given in order that the relative computer times needed for calculating each basis set can be compared. Basis set A is the standard basis set, T(O)DZP, which is described above for the ^{29}Si NMR chemical shift calculations. Only one set of d-functions is applied to all atoms (Table 3). However, Kutzelnigg et al.[47] obtained good results for NMR shieldings if the contraction of the s and p shells was small and a second set of d-type polarization functions was present on silicon and oxygen. Hence, as an alternative to basis set A we adopt their IGLO basis sets (see Table 3) in a locally augmented fashion. Our basis set C uses IGLO-II sets for all atoms in the outer shells of the cluster and IGLO-III sets for the central oxygen atom, the two neighboring silicon atoms, and the second coordination shell of six oxygen atoms (Table 2). The philosophy behind this use of combined basis sets follows from a recent systematic investigation of the influence of calculation parameters upon the calculated ^{17}O NMR shifts of Sil-Y and α-quartz,[15] where it was found, for example, that using an additional IGLO-III basis set for the third shell atoms changed the shielding by less than 0.05 ppm, and using IGLO-II instead of IGLO-III on the second shell atoms changed the shielding by less than 0.5 ppm. However, the results were extremely sensitive to the presence of a second set of d-functions on the central and the first coordination shell atoms.

These observations led to the development of basis set B, which is derived from basis set A by adding a second set of d-functions to the central oxygen atom and the two first shell silicon atoms (TZ2P) and by reducing the contraction of the p-shell on the central oxygen atom (TZp2P) (see Table 3). With a minor increase in the number of basis functions, from 774 to 800 for α-quartz, a major decrease, by about 8 ppm, in the calculated shielding is achieved. The values of $\sigma(\alpha\text{-quartz})$ obtained with the different basis set combinations are listed in Table 2. They can be compared with the estimated value of the experimental absolute shielding of 248 ppm, calculated from the recently reported value of 324 ppm for water molecules[48] and the shift difference of −36.1 ppm[49] required to reference molecular to liquid water. The more traditional ^{17}O shielding scale[49] based on the spin rotation constant of CO yields a shielding of 268 ppm for α-quartz. Considering that our calculations ignore nuclear motion and electron correlation effects, which for H_2O make contributions of −13.2 and +9.7 ppm,[48] respectively, we feel that the calculated *absolute* shieldings are sufficiently close to the experimental value to yield accurate relative shift values. Indeed, for Sil-Y the shift values of the four sites can be reproduced within 2 ppm using α-quartz as a secondary standard.[15] Hence for this study we have also chosen α-quartz as an internal secondary ^{17}O NMR chemical shift reference and applied it accordingly:

$$\delta_{H2O}(\text{cluster}) = \sigma(\alpha\text{-quartz}) + \delta_{H2O}(\alpha\text{-quartz}) - \sigma(\text{cluster})$$

DF chemical shifts were calculated for the Lewis structure using a shell-4 cluster and basis set B was applied. The value of $\sigma(\alpha\text{-quartz})$ was 231.54 ppm. This value is ∼30 ppm lower than the HF result, but it does not necessarily arise from negative contributions to the shielding from electron correlation as it has been shown for water using reliable, but different methods, that a positive effect due to electron correlation (9.6 ppm)[48] is expected. This is in contrast to DF calculations on water that yield a small negative effect even for the B3LYP functional.[44,50] This discrepancy appears to reflect the underestimation of the HOMO-LUMO gap in DF calculations.

^{17}O Electric Field Gradients. Calculations of the electric field gradients on the oxygen nuclei were performed with the Moloch module of the TURBOMOLE code (HF) or with the GAUSSIAN program (DF). The C_Q and η values were extracted from the diagonalized electric field gradient tensor where:

$$C_Q = e^2 q Q_O/h \text{ and } eq = V_{zz}$$

where h is Plancks constant, and

$$\eta = V_{xx} - V_{yy}/V_{zz}$$

where V_{ii} is a diagonal element of the electric field gradient tensor.

Following Eggenberger et al.[51] and Ludwig, Weinhold, and Farrar,[52] the absolute value of the electric quadrupole moment of the oxygen nucleus, Q_O, was calibrated for both types of calculations on the experimental values of C_Q of Sil-Y (HF $Q_O = -2.227$ fm^2, DF $Q_O = -2.242$ fm^2).[15] These are generally applicable values that reproduce the observed C_Q values of α-quartz and coesite within 0.09 MHz.[15] It has also been observed for Sil-Y and α-quartz that calculated C_Q values only vary within a range of 0.02 MHz when a cluster model greater than shell-4 is used indicating that convergence has been achieved. This conclusion can be confirmed for Sil-FER where in Table 8 the results from a shell-4 and a shell-5 model are compared. Only O23 and O45 show larger deviations than expected.

5. Results

^{29}Si NMR. Figure 4 compares the results for the shell-3 calculations of the ^{29}Si NMR chemical shift for the two Sil-FER structures with the Morris experimental spectrum (shift values are given in Table 4). The assignments according to Figure 1 are given above each peak and the lengths of the peaks reflect the multiplicities of each of the sites. The Morris structure gives the correct assignment of the experimental spectrum according to the previous work, but the spread of chemical shifts is too large. The Lewis structure spectrum is extremely close

(44) Cheeseman, J. R.; Trucks, G. W.; Keith, T. A.; Frisch, M. J. *J. Chem. Phys.* **1996**, *104*, 5497−5509.
(45) Schäfer, A.; Horn, H.; Ahlrichs, R. *J. Phys. Chem.* **1992**, *97*, 2571−2577.
(46) Mägi, M.; Lippmaa, E.; Samoson, A.; Engelhardt, G.; Grimmer, A.-R. *J. Phys. Chem.* **1984**, *88*, 1518.
(47) Kutzelnigg, W.; Fleischer, U.; Schindler, M. In *NMR, Basic Principles and Progress*; Springer: Berlin, 1990; Vol. 23, pp 165−261.
(48) Vaara, J.; Lounila, J.; Ruud, K.; Helgaker, T. *J. Chem. Phys.* **1998**, *109*, 8388−8397.
(49) Wasylishen, R. E.; Mooibroek, S.; Macdonald, J. B. *J. Chem. Phys.* **1984**, *81*, 1057.
(50) Rauhut, G.; Puyear, S.; Wolinski, K.; Pulay, P. *J. Am. Chem. Soc.* **1996**, *100*, 6310−6316.
(51) Eggenberger, R.; Gerber, S.; Huber, H.; Searles, D.; Welker, M. *J. Mol. Spectrosc.* **1992**, *151*, 474−481.
(52) Ludwig, R.; Weinhold, F.; Farrar, T. C. *J. Chem. Phys.* **1996**, *105*, 8223−8230.

Table 2. Basis Set Combinations Used in the ^{17}O NMR Chemical Shift and Electric Field Gradient Calculations and the Corresponding Shielding Values of α-Quartz[a]

basis set	central atom (O)	shell-1 (Si)	shell-2 (O)	shell-3 (Si)	shell-4 (O)	shell-5 (Si)	termination (H)	σ(α-quartz) (ppm)	total no. of basis functions used for α-quartz
A	TZP	DZP	TZP	DZP	TZP		DZP	271.0 (shell-4)	774
B	TZp2P	TZ2P	TZP	DZP	TZP	DZP	DZP	262.9 (shell-4)	800
								262.4 (shell-5)	1424
C	III	III	III	II	II		II	269.0 (shell-4)	1047

[a] II and III correspond to basis sets IGLO II and III, respectively.

Table 3. The Number of Gaussian Primitives ( ) and Contracted Basis Functions [ ] for Each Type of Atom Used in the Cluster Models

nomenclature of basis sets used in text	O		nomenclature of basis sets used in text	Si		H	
	(s, p, d)	[s, p, d]		(s, p, d)	[s, p, d]	(s, p)	[s, p]
TZP[43]	10, 6, 1	6, 3, 1	DZP[43]	11, 7, 1	6, 4, 1	4, 1	2, 1
TZp2P[15]	10, 6, 2	6, 4, 2	TZ2P[15]	12, 9, 2	7, 5, 2		
IGLO−II[47]	9, 5, 1	5, 4, 1	IGLO-II[47]	11, 7, 2	7, 4, 2	5, 1	3, 1
IGLO−III[47]	11, 7, 2	7, 6, 2	IGLO-III[47]	12, 8, 3	8, 7, 3		

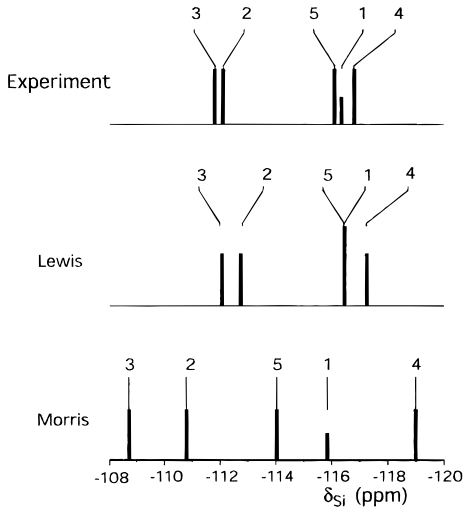

Figure 4. The experimental ^{29}Si NMR isotropic chemical shifts of Sil-FER taken from Morris compared with the calculated shifts of the experimental crystal structures. The T(O)DZP basis set A was used for all the chemical shift calculations. The assignment of the experimental spectrum, given above each peak, was reported by Morris and was obtained from a 2D ^{29}Si NMR correlation experiment. The height of the peaks correctly represents the multiplicity or overlap of the sites.

Table 4. Observed and Calculated ^{29}Si NMR Isotropic Chemical Shifts

Si site[a]	^{29}Si NMR isotropic chemical shift (ppm)		
	exptl shifts[23] (±0.2 ppm)	shifts calcd for the structure of Lewis	shifts calcd for the structure of Morris
Si1	−116.3	−116.6	−115.9
Si2	−112.1	−112.8	−110.8
Si3	−111.8	−112.2	−108.7
Si4	−116.8	−117.4	−119.0
Si5	−116.1	−116.6	−114.0

[a] Labeled according to Figure 1.

to the experimental spectrum (although a negative shift of about 0.5 ppm is observed for the whole spectrum the standard deviation is only 0.14 ppm) with an overlap of sites 1 and 5, which are separated in the experimental spectrum by only 0.2 ppm.

Further support for the accuracy of the Lewis structure can be gleaned from the correlations between the calculated ^{29}Si NMR isotropic chemical shifts and the function of the average Si−O−Si angle for each site (shown by the unfilled symbols in Figure 2). The experimentally determined and calculated chemical shifts for the Lewis structure follow most closely the linear relation between the function of the Si−O−Si angle and the chemical shift (see correlation coefficients).

We conclude from the ^{29}Si NMR chemical shift calculations that the structure determination that most closely represents the local structure of Sil-FER as probed by the NMR experiment is that of Lewis, and hence we should have more confidence in this structure for the ^{17}O NMR shift calculations where the assignment is unknown. The larger spread in chemical shifts seen in the spectrum from the Morris structure is a direct result of the less accurate powder structure determination (as discussed above).

^{17}O NMR. Figure 5 shows the 2-D ^{17}O NMR MQMAS spectrum collected at 14.04 T. In the directly detected dimension five typical quadrupolar broadened line shapes are resolved. The projection along the F1 dimension gives the scaled isotropic spectrum, which is plotted along the *y*-axis. The intensity ratio of the five peaks, including the intensities from the spinning sidebands (not shown), is approximately 1:4:4:8:1 (from left to right) in agreement with the space group *Pnnm*, which has ten different oxygen sites, two with a multiplicity of 4 and eight with a multiplicity of 8. Figure 6 combines, according to Anupõld et al.,[28] the isotropic spectrum from the MQMAS experiment with the field dependent DOR data (Table 5 lists the observed shifts). The data were fitted using ten oxygen sites. The intercept on the *x*-axis corresponds to the isotropic shift for each site and the gradient is proportional to P_Q. The results from this plot are shown in Table 6. The complexity of the spectra render it difficult to follow the field dependence of the shifts, but the excellent agreement between the DOR and MQMAS data leads us to believe that this is the correct fit to all the data. Furthermore, it can be seen from Figure 5 that relatively good agreement, considering the rather poor signal-to-noise ratios of the spectra, is obtained between the anisotropic line shapes obtained from the MQMAS experiment and simulations using the isotropic chemical shifts, and C_Q and η values constrained by the values of P_Q extracted from Figure 6. Here the intensity ratio of the peaks is slightly different, 1:4:3:8:1 from high to low frequency, but this ratio should be treated with caution due to the poor signal-to-noise ratio of the two outer peaks.

The assignment of this ^{17}O NMR spectrum is especially difficult due to its complexity and the small dispersion in the

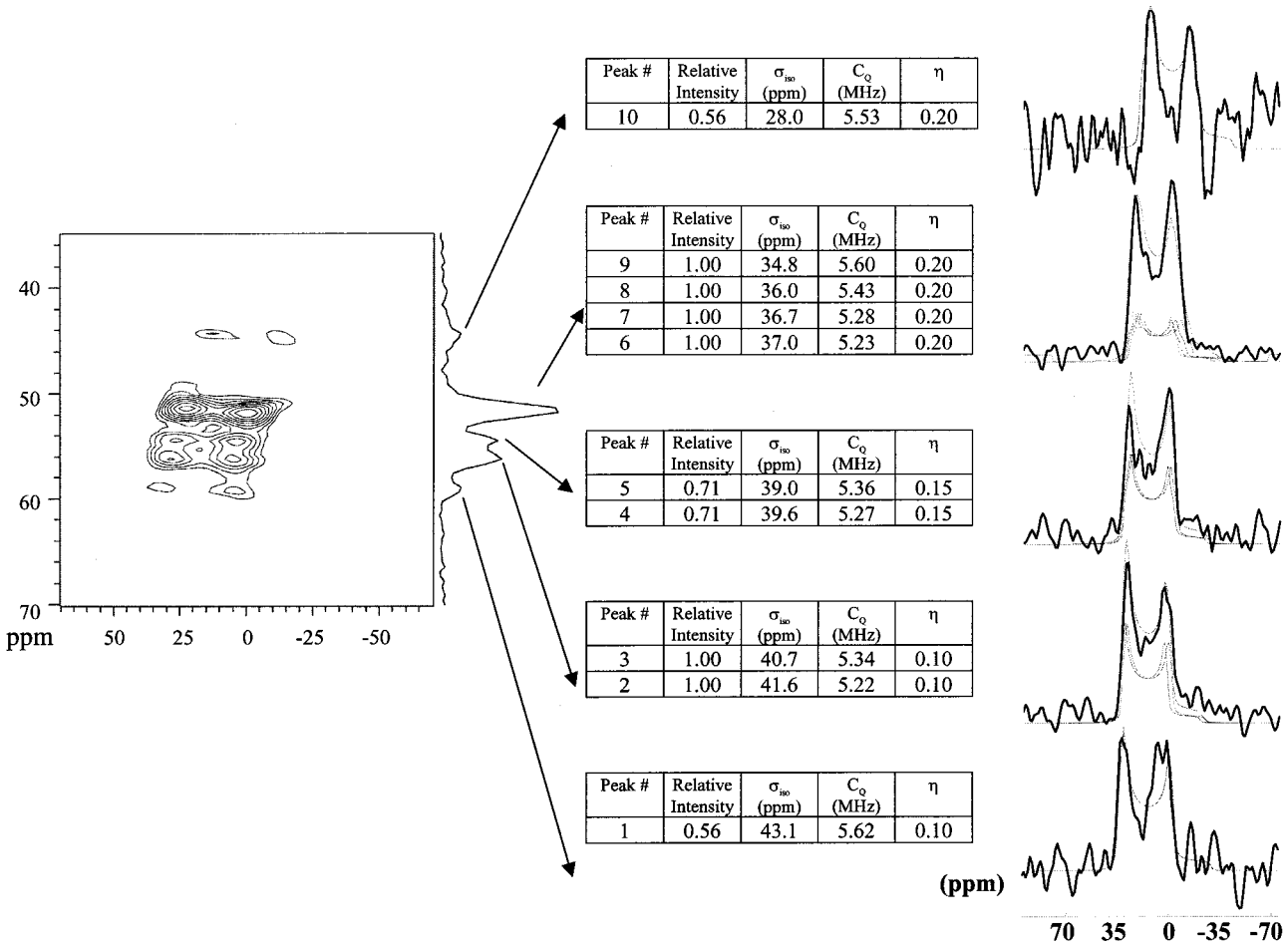

Peak #	Relative Intensity	σ_{iso} (ppm)	C_Q (MHz)	η
10	0.56	28.0	5.53	0.20

Peak #	Relative Intensity	σ_{iso} (ppm)	C_Q (MHz)	η
9	1.00	34.8	5.60	0.20
8	1.00	36.0	5.43	0.20
7	1.00	36.7	5.28	0.20
6	1.00	37.0	5.23	0.20

Peak #	Relative Intensity	σ_{iso} (ppm)	C_Q (MHz)	η
5	0.71	39.0	5.36	0.15
4	0.71	39.6	5.27	0.15

Peak #	Relative Intensity	σ_{iso} (ppm)	C_Q (MHz)	η
3	1.00	40.7	5.34	0.10
2	1.00	41.6	5.22	0.10

Peak #	Relative Intensity	σ_{iso} (ppm)	C_Q (MHz)	η
1	0.56	43.1	5.62	0.10

Figure 5. 2D ^{17}O NMR MQMAS spectrum of Sil-FER showing in the vertical direction the MQMAS scaled isotropic spectrum (projection along the *y*-axis) and in the horizontal direction the anisotropic line shapes for the five resolved peaks. Simulations of each of the anisotropic line shapes are shown on the right of the figure and are fitted using the P_Q values obtained from the field dependence of the ^{17}O NMR experiments (Table 6 and Figure 6) to constrain the values of C_Q and η.

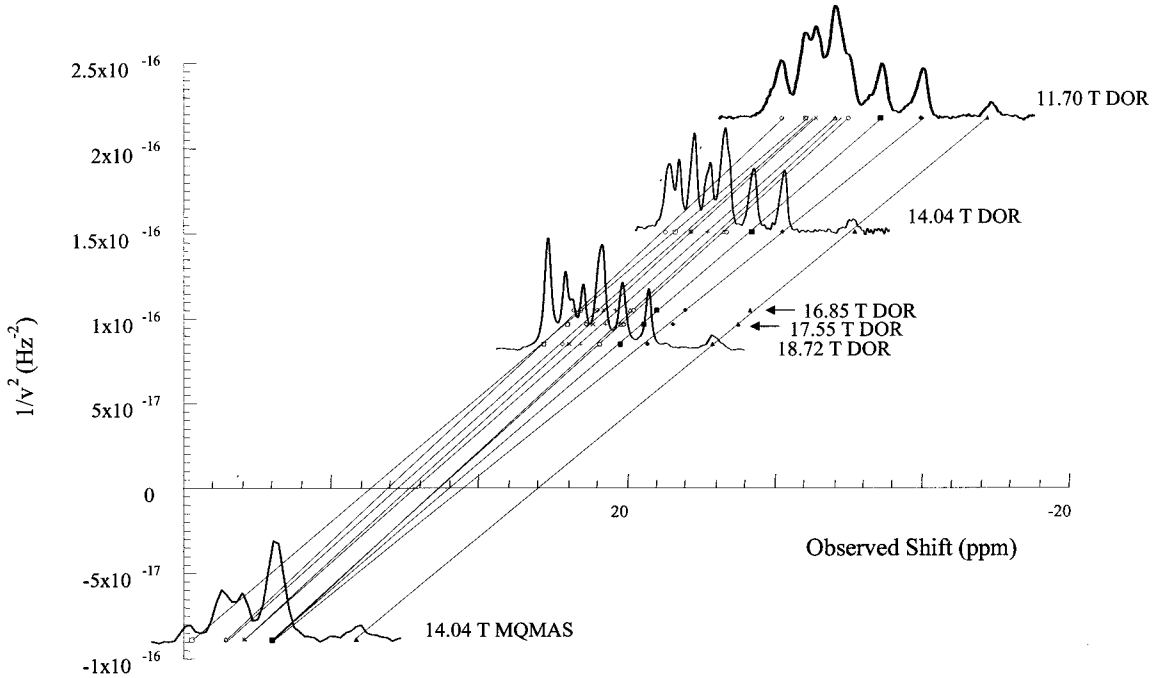

Figure 6. Field dependence of the ^{17}O NMR DOR and MQMAS data plotted according to Samoson et al.[28]

values of the isotropic chemical shift and electric field gradient. Figure 7 shows the graph of calculated C_Q values (using experimental structures and shell-4 HF/A calculations) versus the Si−O−Si angle at each oxygen for several structures. The solid line represents a modified version of the Townes−Dailey model that Grandinetti et al. used for assigning the ^{17}O NMR

Table 5. Field Dependence of the ^{17}O NMR Chemical Shift Measured Using DOR and MQMAS

field strength (T)	^{17}O NMR Larmor freq υ (Hz)	scaled $1/\upsilon^2$ used in Figure 6 (Hz^{-2})	obsd ^{17}O NMR chemical shifts (ppm) from DOR (±0.2) and MQMAS (±0.3)									
			peak 1	peak 2	peak 3	peak 4	peak 5	peak 6	peak 7	peak 8	peak 9	peak 10
18.72	1.0847e^8	8.4995e^{-17}	27.49	27.49	25.87	25.24	24.23	22.53	22.53	20.64	18.20	12.34
17.55	1.0169e^8	9.6701e^{-17}	25.40	25.40	23.70	23.10	22.00	20.60	20.30	18.50	15.90	10.00
16.85	9.7604e^7	1.0497e^{-16}	24.27	24.80	22.70	22.17	21.07	19.76	19.50	17.40	14.80	8.94
14.04	8.1356e^7	1.5108e^{-16}	15.70	16.61	14.28	14.28	12.80	11.30	11.10	8.80	6.00	−0.50
11.70	6.7760e^7	2.1780e^{-16}	3.94	6.10	3.90	3.00	1.24	1.24	0.10	−2.82	−6.50	−12.50
14.04	8.1356e^7	−8.8868e^{-17} [a]	59.30	56.20	56.20	54.50	54.50	52.00	52.00	52.00	52.00	44.40

[a] MQMAS Larmor frequency is scaled by a factor of −(10/17) according to Anupõld et al.[28]

Table 6. Parameters Extracted from Field-Dependent ^{17}O NMR DOR and MQMAS Data (Figure 6)

peak no.	isotropic chemical shift ±0.3 (ppm)	quadrupolar product ±0.03 (MHz)
1	43.1	5.62
2	41.6	5.22
3	40.7	5.35
4	39.6	5.29
5	39.0	5.38
6	37.0	5.27
7	37.0	5.32
8	35.9	5.46
9	34.8	5.64
10	28.0	5.57

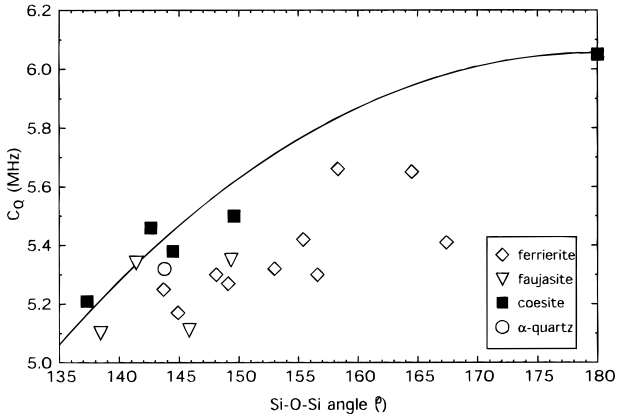

Figure 7. A graph of the calculated ^{17}O NMR C_Q values (observed structures and shell-4 HF/A calculations) versus the Si−O−Si bond angle at each oxygen for various reference materials[15] and the Lewis crystal structure of Sil-FER. The semiempirical correlation developed by Grandinetti et al.[12] is shown by the solid line, demonstrating that this kind of simple correlation between ^{17}O NMR C_Q values and the Si−O−Si bond angle is not generally applicable.

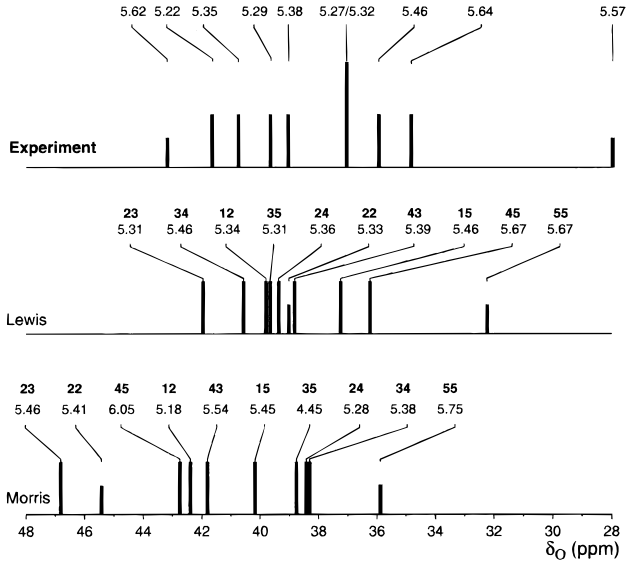

Figure 8. The experimental ^{17}O NMR isotropic chemical shifts extracted from Figure 6 compared with the calculated shifts for the two crystal structures. The basis set B was used for all the chemical shift calculations. Above each peak the corresponding experimental or calculated P_Q values are given in normal type, and for the calculated spectra, the assignments of each peak according to the scheme used in Figure 1 are given in bold. The height of the peaks correctly represents the multiplicity or overlap of the sites.

spectrum of the mineral coesite (eq 31 of ref 12). It is clearly seen that only the data calculated for coesite follow the modified Townes−Dailey model, while the other data show only a weak dependence of C_Q with the Si−O−Si bond angle, which is not significant enough to be used to assign the Sil-FER spectrum. A Townes−Dailey correlation between the asymmetry parameter of the electric field gradient tensor and the Si−O−Si bond angle has also been proposed, but the combination of the poor signal-to-noise ratio of the anisotropic line shapes from the MQMAS data and the small variation in the values of η rules out this kind of correlation for our Sil-FER data. No simple correlations are known to exist between any geometric parameter and the ^{17}O NMR isotropic chemical shift for bridging oxygens in tectosilicates,[14] unlike for ^{29}Si NMR shifts. The correlation proposed between the Si−O−Al bond angle and the ^{17}O NMR shift and used for assigning the ^{17}O spectra of zeolites Na-A and Na-LSX[9] is not supported for Si−O−Si bridging oxygens by the studies on Sil-Y[11] and silicate species.[14] We believe that if such a correlation does exist it can be rationalized only in terms of the contribution to the shift from the Si−O bonding pairs of electrons. However, the two lone pairs of electrons on oxygen are expected to make the largest contribution to the ^{17}O shielding, but due to their large polarizability and significant spatial extension, the contribution they make to the shieldings is obviously difficult to predict from simple models.

In ref 11 it was demonstrated that quantum mechanical cluster calculations of ^{17}O NMR chemical shielding constants can now reproduce relatively accurately the experimentally determined spectrum of Sil-Y. The principal factor in determining the accuracy of the calculations, if the cluster size is sufficiently large, is the accuracy of the experimental crystal structure determination used in defining the cluster model. Hence, Figure 8 shows the comparison of the ^{17}O NMR spectra of Sil-FER calculated for the two structures using shell-4 clusters and basis set B with the experimental ^{17}O NMR spectrum (shifts given in Table 7). The experimental and calculated values of P_Q for each peak are given in normal type above the peaks and the assignments from the calculated chemical shifts are given in bold (C_Q and η values are given in Table 8). There are several general observations that can be made immediately: (1) the spread of chemical shifts for both structures is less than that experimentally determined. This was seen previously for Sil-Y

Table 7. Calculated ^{17}O NMR Isotropic Chemical Shifts (ppm) for Different Structures

	Lewis					Morris
atom	shell-4 HF/A	shell-4 HF/C	shell-4 HF/B	shell-4 DF/B	shell-5 HF/B	shell-4 HF/B
O12	39.5	40.2	39.8	39.1	39.8	42.4
O15	36.8	37.1	37.3	35.6	36.6	40.2
O22	39.4	39.8	39.0	37.9	39.0	45.4
O24	39.2	39.7	39.4	38.1	38.8	38.4
O23	42.5	42.1	42.0	41.1	41.5	46.8
O35	40.3	38.9	39.7	38.4	38.9	38.8
O34	39.9	41.2	40.6	40.5	40.3	38.3
O43	38.3	39.2	38.8	37.1	38.4	41.8
O45	34.8	35.5	36.3	34.6	35.5	42.8
O55	30.9	31.3	32.3	29.7	31.6	35.9

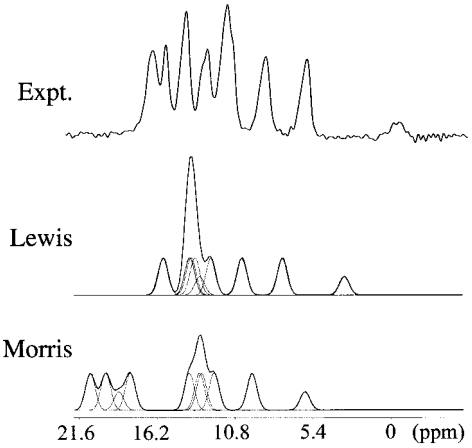

Figure 9. A comparison of the experimental ^{17}O NMR DOR spectrum of Sil-FER at 14.04 T with the simulations of the theoretical spectra for the two crystal structures using the isotropic chemical shifts and P_Q values obtained from Tables 7 and 8. A Gaussian broadening of 60 Hz was applied to each of the calculated peaks in the simulated spectrum. This is comparable to the experimental line widths.

and is still not fully understood; (2) site O55 of multiplicity 4 is located at the lowest frequency of the calculated spectra and O22, the other site of multiplicity 4, is located toward the center of the calculated spectra; (3) the spread of calculated P_Q values for the Lewis structure (0.36 MHz) is significantly closer to the experimental range (0.42 MHz) than the Morris structure (1.3 MHz); and (4) typically the larger values of P_Q are obtained for the lower frequency peaks. This was also observed for Sil-Y[11] and Coesite.[12]

The calculated spectra from both crystal structures are in agreement about the assignment of the peak at 28 ppm to O55, but the other multiplicity 4 peak is difficult to assign. According to the relative intensities of the peaks in the isotropic spectrum obtained from the MQMAS experiment, we would predict that the peak on the far left side of the spectrum was site O22. None of the calculated spectra would predict this. However, it should be remembered that first, the low signal-to-noise ratio of the MQMAS data means that the integrated intensities of the smaller peaks are subject to larger relative errors, and second, the simulations of the anisotropic slices of the MQMAS data gave slightly different relative intensities of 1:4:3:8:1, which could be consistent with O22 appearing in the center of the spectrum. The DOR intensities would appear not to be in agreement with this latter interpretation of the data; however, based on the DOR data from Sil-Y where all the sites had the same multiplicity yet the peaks were of significantly different intensities, we should be extremely careful in interpreting intensities due to

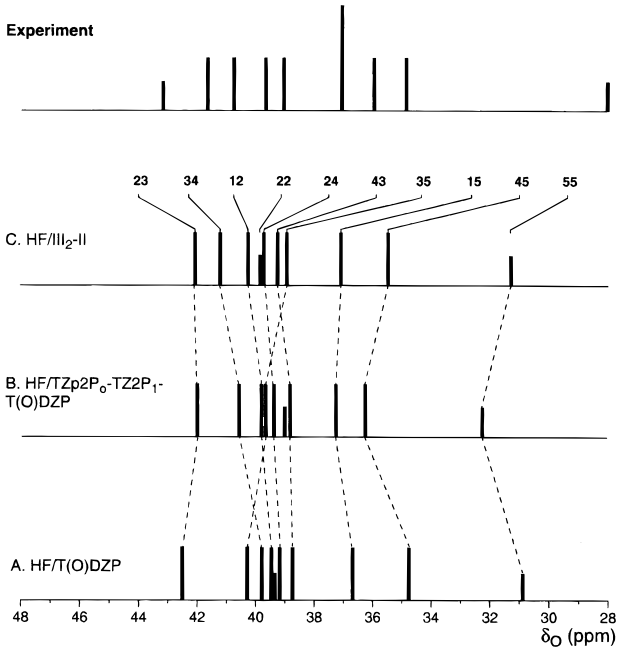

Figure 10. The experimental ^{17}O NMR isotropic chemical shifts extracted from Figure 6 compared with the shell-4 cluster calculated shifts extracted from the Lewis structure of Sil-FER. Different basis sets were used, as indicated. The calculated spectra are assigned according to the scheme used in Figure 1. Dashed lines join the peaks with the same assignments except for O22, where for clarity, the height of the peak can be used to follow its evolution.

effects of chemical shift anisotropy, relaxation, and possibly site selective ^{17}O enrichment.

Comparing the calculated ^{17}O NMR spectra of Sil-FER with the experimental results it is clear that it is impossible to make a complete assignment of the spectrum as the calculations do not reproduce the experimental spectrum as closely as for the ^{29}Si NMR data. From the experimental point of view this can be understood as first, the ^{17}O NMR spectrum contains a larger number of peaks with very similar values of P_Q in a small shift range, and second, due to the presence of the quadrupolar interaction, it is necessary to extrapolate the field dependence of the ^{17}O NMR observed shifts to infinite magnetic field strength to obtain the isotropic shift. However, as Figure 9 shows, this latter source of error can be negated by simulating an experimentally observed ^{17}O NMR spectrum (here a DOR spectrum at 14.04 T) using the calculated values of the isotropic chemical shift and the values of P_Q. It is clear that the chemical shift and electric field gradient calculations for both structures of Sil-FER still have problems in reproducing the high-frequency side of the ^{17}O NMR spectrum. However, the agreement between the experimental and simulated spectrum for the Lewis structure is significantly better than that for the Morris structure, showing clearly the three lines at the low frequency side of the spectrum and close spacing of the peaks in the central region. From these findings we conclude that it is possible to assign three oxygen sites O55, O45, and O15 according to the Lewis spectrum in Figure 8. The other peak relatively well separated from the central peaks on the left side of the spectrum cannot be definitively assigned to O23 as its intensity and P_Q value are inconsistent with the experimental results.

It is difficult to really understand why the calculations of the ^{29}Si NMR chemical shifts are of superior quality to those of ^{17}O, although it is true that the experimental NMR shift range of ^{17}O ($>$1000 ppm) is considerably greater than that of ^{29}Si ($>$100 ppm) and thus for the same relative accuracy the absolute

Table 8. Calculated ^{17}O NMR Quadrupolar Coupling Constants and Asymmetry Parameters [C_Q (MHz)/η] for Each Oxygen Site

	Lewis					Morris
atom	shell-4 HF/A	shell-4 HF/C	shell-4 HF/B	shell-4 DF/B	shell-5 HF/B	shell-4 HF/B
O12	5.31/0.04	5.24/0.05	5.34/0.04	5.28/0.04	5.36/0.04	5.18/0.03
O15	5.42/0.10	5.34/0.11	5.45/0.10	5.37/0.09	5.44/0.10	5.37/0.29
O22	5.27/0.10	5.18/0.12	5.32/0.10	5.22/0.10	5.34/0.08	5.38/0.17
O24	5.32/0.06	5.24/0.06	5.36/0.05	5.29/0.05	5.38/0.06	5.27/0.10
O23	5.17/0.14	5.08/0.15	5.30/0.13	5.15/0.12	5.24/0.14	5.43/0.18
O35	5.25/0.18	5.15/0.19	5.29/0.17	5.22/0.16	5.29/0.17	4.36/0.36
O34	5.42/0.09	5.40/0.09	5.45/0.08	5.40/0.08	5.44/0.07	5.37/0.09
O43	5.30/0.18	5.22/0.17	5.36/0.17	5.31/0.17	5.36/0.18	5.52/0.15
O45	5.54/0.06	5.48/0.06	5.67/0.05	5.54/0.06	5.56/0.05	6.02/0.16
O55	5.64/0.09	5.56/0.11	5.66/0.09	5.56/0.09	5.66/0.03	5.70/0.22

error for ^{17}O shifts should be greater. We do not believe that the errors arise from the choice of basis sets for the two atoms as, even though oxygen is the more electronegative component in SiO_2, and hence the distribution of the electron density is more important, we have already compensated for this by using more elaborate basis sets on oxygen. What may contribute to the difficulty in calculating ^{17}O NMR shifts with the same accuracy as ^{29}Si NMR shifts is the fact that oxygen atoms undergo larger vibrational amplitudes than silicon atoms in zeolite lattices. These fluctuations will vary from site to site depending upon the different constraints of the lattice. Currently, vibrational contributions can be calculated only for small molecules[48] and thus they are ignored in our calculations, so inducing larger errors in the shieldings of ^{17}O than ^{29}Si.

To try to estimate the accuracy of the ^{17}O NMR shift and electric field gradient results, further calculations were performed using the crystal structure of Lewis to attempt to ascertain which parameters most significantly influenced the data. The values of δ and C_Q and η are given in Tables 7 and 8, respectively.

Figure 10 shows the results from shell-4 clusters taken from the Lewis structure using different basis set combinations. The similarity of the predicted spectra in Figure 10 is striking, indicating that modest variations of the basis set do not influence significantly the calculations. The only differences that occur are at the centers of the spectra, where within a range of approximately 2 ppm, six peaks are predicted. We believe that the kind of accuracy needed to be sure of the assignment of these 6 peaks is beyond the current limits of our chemical shift calculations. An estimation for the error on the calculated values of P_Q (C_Q and η values are given in Table 8) is approximately 0.15 MHz.

Other tests of the calculations were performed. A shell-5 cluster calculation taken from the Lewis structure with basis set B is shown in Figure 11. Slight differences in the assignments are observed between the shell-4 and shell-5 cluster models only at the centers of the spectra. This is reassuring evidence that above the 4th shell the size of the cluster is no longer important in determining the ^{17}O NMR chemical shift of Sil-FER in accordance with that observed for Sil-Y.[15] From these results we can estimate the error in the calculated chemical shift due to using a shell-4 cluster model to be less than 1 ppm, which is significantly lower than that arising from changing the structural model (see Figure 8).

In Figures 8 and 10 it can be seen that the range of calculated ^{17}O NMR chemical shifts is less than the experimentally determined spread. This was also observed for Sil-Y when the chemical shifts were calculated using the HF method. When DF chemical shift calculations were performed the spread increased, but the relative positions of the four oxygens remained the same. Hence, Figure 11 compares the results from the DF and HF chemical shift calculations on a shell-4 cluster taken from the Lewis structure and using basis set B. Indeed the spread in the chemical shifts is increased when DF calculations are performed, approaching more closely the experimentally observed shift range. In addition, the order of the peaks is identical for the two methods, supporting our assignment of sites O55, O45, and O15 according to Figure 8 using the Lewis structure. Again it can be seen that the change induced by using the HF chemical shift calculations instead of the DF calculations is not significant in comparison to the change caused by altering the structure of the cluster.

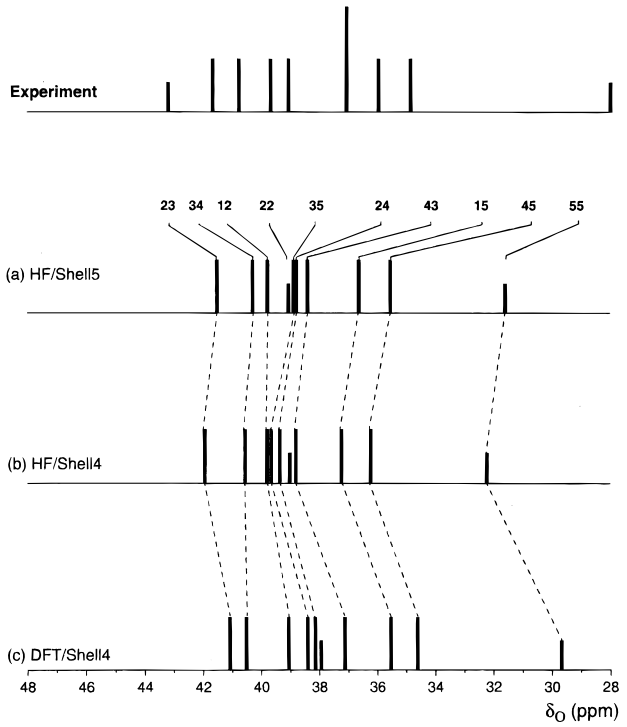

Figure 11. The experimental ^{17}O NMR isotropic chemical shifts extracted from Figure 6 compared with calculations using clusters extracted from the Lewis structure. All calculations used basis set B. ^{17}O NMR chemical shift calculations were performed using (a) shell-5 and (b) shell-4 clusters and the HF method and (c) a shell-4 cluster and the DF method. The calculated spectra are assigned according to the scheme used in Figure 1. Dashed lines join the peaks with the same assignments except for O22, where for clarity, the height of the peak can be used to follow its evolution.

6. Conclusions

We have shown that it is possible to obtain high-resolution ^{17}O NMR spectra from a complex zeolitic material, Sil-FER, and have extracted the isotropic chemical shifts and P_Q values. ^{29}Si NMR chemical shift calculations have very accurately reproduced the experimental shifts and assignment of Sil-FER.

The calculated spectrum is shown to be extremely sensitive to the structural model, and thus can be used to judge the accuracy of a crystal structure.

Calculations of the ^{17}O NMR electric field gradient tensors and the isotropic chemical shifts of Sil-FER are presented. Partial assignment of the experimental ^{17}O NMR spectrum is possible based upon the isotropic chemical shifts. Only a weak dependence was observed between C_Q and the Si−O−Si bond angle and none between the isotropic chemical shift and any simple geometric function. Calculations performed using different methods (HF and DF), a variety of basis sets, and clusters of different sizes indicate that the ^{17}O chemical shift calculations are accurate to approximately 2.0 ppm, and that the primary source of error is the structural model used in the calculation. The sensitivity of the calculations to the structure can be seen, for example, by considering O55. The difference between the calculated ^{17}O NMR shifts for the Morris and Lewis structures is 3.6 ppm, whereas the Si5−O55−Si5 bond angles only changes by 1.2°. We believe that three peaks in the ^{17}O NMR spectrum of Sil-FER can be definitively assigned to O55, O45, and O15 according to the Lewis structure spectrum in Figure 8. The shift difference between the remaining peaks is too small for accurate assignment. The position of site O22 remains elusive. From the experimental data we expect this peak to be at the highest frequency whereas the calculations predict it to be toward the center of the spectrum. This problem remains unresolved as the intensities from DOR and MQMAS are not sufficiently reliable due to effects such as relaxation, chemical shift anisotropy, and site selective ^{17}O enrichment.

This sample has demonstrated the current limits of both the experimental NMR techniques and the chemical shift and electric field gradient calculations and clearly shows that ^{29}Si and ^{17}O NMR chemical shifts are extremely sensitive structural probes. We believe that the combination of experimental and calculated chemical shifts can be used to judge the accuracy of oxide crystal structures in general. Finally, we predict that experimental and calculated chemical shifts will be included into diffraction data structural refinement models enabling more accurate structures to be determined.

Acknowledgment. This work and L.M.B. were supported by the MRSEC Program of the National Science Foundation under award No. DMR-9632716, the CNRS, and the Région Pays de Loire. R.D. would like to acknowledge the EPSRC (UK) and funding from the UK HEFCE for a JREI grant for the CMX 600 spectrometer. A.S., T.A., and A.R. are supported by a NATO linkage grant 1 1312 0154 and would like to acknowledge the Estonian Science Foundation. Use of the NMR facilities at the NHMFL, Florida, Technical University, Munich, Germany, and the Frankfurt University Center for Biomolecular NMR, Germany, is greatly appreciated. We are also grateful to the Deutsche Forschungsgemeinschaft project Mi 390/5-2 and to Professor Dr. D. Michel, University of Leipzig, Germany, for providing 750 MHz solid-state NMR time. The computational part of this project was supported by the Max-Planck-Gesellschaft, the Fonds der Chemischen Industrie, and the Max Buchner-Forschungsstiftung. Finally, we would also like to thank Dr. S. Weigel for synthesizing the sample of Sil-FER.

JA993339Y